Synthesis and Reactivity in Inorganic, Metal-Organic, and Nano-Metal Chemistry

ISSN: 1553-3174 (Print) 1553-3182 (Online) Journal homepage: http://www.tandfonline.com/loi/lsrt20

Hierarchical self-assembly of flower-shaped CuO with high photocatalysis efficiency for degradating Rhodamine B

Xinqing Ge, Hanmei Hu, Qiang Zheng & Mei Sun

To cite this article: Xinqing Ge, Hanmei Hu, Qiang Zheng & Mei Sun (2016): Hierarchical self-assembly of flower-shaped CuO with high photocatalysis efficiency for degradating Rhodamine B, Synthesis and Reactivity in Inorganic, Metal-Organic, and Nano-Metal Chemistry, DOI: 10.1080/15533174.2015.1137018

To link to this article: http://dx.doi.org/10.1080/15533174.2015.1137018

Accepted author version posted online: 22 Feb 2016.

Hierarchical self-assembly of flower-shaped CuO with high photocatalysis efficiency for degradating Rhodamine B

Xinqing Ge[a], Hanmei Hu[a,b]*, Qiang Zheng [a], Mei Sun[a]

[a]*Key Laboratory of Functional Molecule Design and Interface Process, Anhui University of Architecture, Hefei, 230601, China*

[b]*School of Materials and Chemical Engineering, Anhui University of Architecture, Hefei, 230601, ,China*

* Corresponding author. *E-mail address*: hmhu@ustc.edu (H.M. Hu)

Abstract

The flower-shaped CuO with hierarchical microstructures were successfully synthesized through an ultrasound-assisted aqueous chemical method. The comparative experiment results show that the phase and morphology of as-obtained products are greatly affected by the volume of ammonia and the time for keeping ultrasonic irradiation, respectively. The prepared CuO microflowers assembled by nanosheets with needle-like tips exhibit a much higher activity than the commercial CuO for degradating Rhodamine B (RhB). Additionally, the photocatalytic performance of as-prepared hierarchical CuO microflowers was also evaluated through the degradation of Methylene blue (MB) and Methyl orange (MO) under the same conditions.

Keywords: Copper oxide; Hierarchical self-assembly; Microstructure; Organic pollutants; Photocatalytic activity

1. Introduction

Recently, many efforts have been focused on the hierarchical assembly of nanoscale building blocks (nanoparticles, nanorods or nanosheets, etc.) into ordered superstructures or higher level sophisticated architectures. [1-4] Superstructures or hierarchical assembly can exhibit collective physical and chemical properties which are not found on the level of individual nanoblocks. [5-6] Copper oxide (CuO), as an important p-type semiconductor with a narrow band gap of 1.2eV, [7] has attracted a great interest in which not only its excellent physical and chemical properties but also its potential applications in many fields, such as, gas sensor material,[8] anion material, [9] catalyst, [10,11] lithium ion battery [12] and supercapacitor. [13]

Numerous efforts have been made to prepare CuO micro/nano hierarchical architectures with special properties. Dendrite-shaped CuO hollow micro/nanostructures have been synthesized via a Kirkendall-effect-based approach, acting as a high-performance anode material for lithium-ion batteries.[14] Perpendicularly cross-bedded CuO microstructures with good gas sensitivities targeting at ethanol and acetone have been prepared through a precursor-based route.[15] Urchin-like core-shell CuO assembled by nanorods has been hydrothermally synthesized in assistance of poly(ethylene glycol) (PEG), which exhibits wide biosensor capability toward H_2O_2.[16] Flower-like CuO nanostructures with room-temperature ferromagnetism were prepared by the coprecipitation method with postannealing in air at different temperatures. [17] CuO microflowers composed of nanosheets have been fabricated in

ammonia solution at 90-180 ºC, exhibiting effective catalytic activity on the decomposition of ammonium perchlorate.[18] Recently, Uniform and well-defined CuO cauliflowers have been prepared through a hydrothermal route, showing a much higher activity than the irregular CuO for the degradation of Rhodamine B (RhB). [11]

However, many reported methods have ineluctable high-cost and time-consuming, is unfriendly to the environment. Hence, it's still a challenge to design a facile and green preparation method to obtain CuO nano/micromaterials. In this work, well-defined hierarchical CuO flower-shaped microstructures were successfully fabricated by an ultrasound-assisted aqueous chemical method. Photocatalytic results indicate that the obtained CuO flowers exhibit excellent photocatalytic activity for the degradation of RhB in the presence of H_2O_2 under tungsten lamp irradiation.

2. Experimental

2.1 Materials

All chemicals used in this study were analytical grade and were not subjected to additional purification. Copper acetate monohydrate ($Cu(CH_3COO)_2 \cdot H_2O$), ammonia ($NH_3 \cdot H_2O$) and hydoxylamine hydrochloride ($NH_2OH \cdot HCl$), which were purchased from Shanghai guoyao chemical reagent LTD.

2.2 Synthesis of flower-shaped CuO

In a typical procedure, 1mmol $Cu(CH_3COO)_2 \cdot H_2O$ and 0.5mmol $NH_2OH \cdot HCl$ were dissolved in 60 mL distilled water under stirring. After continuous stirring for 10 minutes, 0.5mL ammonia was added to the mixed solution under stirring to form precursor solution. Afterwards, the precursor solution was transferred into a 100 mL autoclavable bottle sealed with attached screw cap to form a closed system, which was put into a sonication bath with the water temperature of 60 ºC and irradiated for 40 minutes by ultrasonic wave. Subsequently, the bottle was taken out carefully and cooled down to room temperature naturally. The black precipitate was observed and filtered out, washed several times with distilled water and absolute ethanol, and then dried in a vacuum at 60 ºC for 6h.

2.3 Photocatalytic experiments

Photocatalytic experiments were performed in a reflux system (shown in Fig. 1). A self-made double walled glass vessel with cooling water was placed on a magnetic stirrer, in which a beaker containing dye and catalyst suspension was put, so as to decrease the thermal effect. A 500 W tungsten lamp was used as the light resource. Prior to photocatalytic studies, the mixture of 25mg catalyst and 50mL organic dye (10mg/L) was stirred for 60min in dark to reach the balance of adsorption and desorption on the surface of catalyst. Then the suspension was exposed to tungsten lamp light with continuous stirring in the presence of 0.1mL hydrogen peroxide (H_2O_2). At the specific time interval, the dispersion was sampled (4mL) and centrifuged for 3 min to separate the catalyst. The supernatant of dyes were put into a quartz cell. The

concentration of the corresponding dye was measured with a UV-5500PC spectrophotometer.

2.4 Instrument and characterization

The chemical reactions were implemented in an ultrasonic generator (Kunshan Co., KQ-50, 50 W, 40 kHz). The X-ray diffraction patterns of as-prepared products were obtained by X-ray diffraction (XRD) using a Bruker D8 Advance X-ray diffractometer (40 kV, 40 mA) equipped with graphite monochromatized Cu K_α radiation (λ=0.15406 nm). The surface morphology and size of as-obtained samples were measured on a field emission scanning electron microscope (JEOL JSM-6700F) and a transmission electron microscope (H-7650). UV-Vis diffuse reflectance spectra (DRS) were recorded on a UV-Vis spectrophotometer (Solidspec-3700 DUV) at room temperature.

3. Results and discussion

3.1 Characterization of flower-shaped CuO microstructures

The crystal structure and phase purity of the prepared products were determined by using X-ray diffraction (XRD). Fig. 2 shows the XRD pattern of the as-prepared sample. All the peaks can be clearly indexed to cubic CuO crystal planes, which were consistent with the standard data for CuO (JCPDS 80-1916). In addition, no other obvious impurities are observed, such as $Cu(OH)_2$ and Cu_2O. The intense and strong reflection peaks suggest that the products are highly crystalline.

Fig. 3(a) and (b) show the FESEM images of CuO samples prepared by ultrasonic radiation for 40 min. It can be seen that the as-prepared CuO products are mainly composed of uniformly elegant flower-like microstructures, which were produced in large quantities. The sizes of CuO microflowers are estimated to be 2-3 μm. These flower-like architectures are self-assembled by nanosheets with needle-like tips radiating from their center. The inset figure in Fig. 3(b) clearly shows a typical peony-like particle. The thicknesses of nanosheet building units are in the range of 10-20 nm and the widths of middle parts of these nanopetals are about 300-400nm. Fig. 3(c) and (d) are the representative TEM images of the obtained CuO sample, which still preserve the shapes of flower after the ultrasonic treatment. Fig. 3(d) is a high-magnification image of many flower petals, indicating that the needle-like tips grow out from the middle region of CuO nanosheets, and the width of each sheet-like nanopetal gradually decreases from the bottom toward the tip.

3.2 Influencing factor and growth mechanism

In the present designed reaction system, the phases of obtained products are greatly affected by the adding amounts of ammonia ($NH_3 \cdot H_2O$). The XRD patterns of comparative experiments are presented in Fig. 4(a). The introduction of $NH_3 \cdot H_2O$ and its dosage are crucial for the formation of CuO phase. If no $NH_3 \cdot H_2O$ is added into the reaction system keeping other conditions unchanged, the obtained products are $Cu(OH)_2$ (JCPDS 72-0140) as well as trace amounts of Cu_2O (marked by "&"). It is suggested that $NH_2OH \cdot HCl$ mainly act as precipitation

reagent for Cu^{2+} ions to generate $Cu(OH)_2$ precipitate in the absence of $NH_3 \cdot H_2O$. Simultaneously, a little bit of Cu^{2+} ions in the solution are reduced to Cu^+ by $NH_2OH \cdot HCl$, generating Cu_2O impurity phase in the products. When the volume of ammonia is 0.3mL, the obtained products are the mixture of $Cu(OH)_2$, Cu_2O and CuO (marked by "*"). While the volume of ammonia is added up to 0.5 mL, pure CuO phase can be achieved (Fig. 1). In addition, ultrasonic treatment is indispensable for growing CuO microflowers in the present system. In the absence of ultrasonic irradiation, pure CuO can not be obtained. Fig. 4(b) present the XRD pattern of product prepared without ultrasonic treatment keeping other condition constant, which exhibit that the product is the mixture of CuO and Cu_2O.

In the present reactive system, $NH_3 \cdot H_2O$ is a weak base ($K_b=1.8\times10^{-5}$), but $NH_2OH \cdot HCl$ is an acid reagent ($K_a=1.1\times10^{-6}$). In the absence of ammonia, Ac^- ions in the aqueous solution hydrolyze to produce OH^- [Eq. 1]. New-produced OH^- ions react with $NH_2OH \cdot HCl$, generating NH_2OH [Eq. 2]. As a weak base ($K_b=9.1\times10^{-9}$), NH_2OH continue to hydrolyze to produce OH^- [Eq. 3], which combine with Cu^{2+} to form $Cu(OH)_2$ precipitate [Eq. 4]. When the appropriate amount of ammonia is added, abundant OH^- ions are produced owing to the dissociation of $NH_3 \cdot H_2O$ [Eq. 5]. Then, the preformed $Cu(OH)_2$ combine with OH^- ions to form $Cu(OH)_4^{2-}$ complexes [Eq. 6]. Finally, $Cu(OH)_4^{2-}$ coordinate compounds will dehydrolyze to generate CuO products [Eq. 7]. The whole reaction process can be described as follows:

$$Ac^- + H_2O = HAc + OH^- \quad (1)$$

$NH_2OH{\cdot}HCl + OH^- = NH_2OH + H_2O + Cl^-$ (2)

$NH_2OH + H_2O = [NH_3OH]^+ + OH^-$ (3)

$Cu^{2+} + 2OH^- = Cu(OH)_2$ (4)

$NH_3{\cdot}H_2O = NH_4^+ + OH^-$ (5)

$Cu(OH)_2 + 2OH^- = Cu(OH)_4^{2-}$ (6)

$Cu(OH)_4^{2-} = CuO + H_2O + 2OH^-$ (7)

To investigate the growth process of flower-like CuO. Time-dependent comparative experiments were carried out while keeping other conditions unchanged, which was illustrated in Fig. 5. Fig. 5(a) indicates the corresponding XRD patterns of products obtained when the ultrasonic irradiation time is 0 min, 5 min and 20 min, respectively. Before the ultrasonic irradiation, light blue $Cu(OH)_2$ products (JCPDS 72-0140) as well as trace amounts of Cu_2O impurity phase (marked by "&") have been detected. When the ultrasonic irradiation time is 5 min, the products are the mixture of $Cu(OH)_2$, Cu_2O and CuO (marked by "*"). While the ultrasonic irradiation time is extended to 20 min or above, pure CuO phase can be obtained. The morphology of $Cu(OH)_2$ are nanobelts and belt-like aggregates (Fig. 5b). Fig. 5(c) give the picture of products obtained when the ultrasonic irradiation time is 5 min, indicating that the products are composed of $Cu(OH)_2$ nanobelts and CuO shuttle-shaped nanostructures (indicated by the white dashed circle in Fig. 5(c)). When the irradiation time is 10 min, large quantities of CuO nanoshuttles are generated. It can be seen that some nanoshuttles have secondary generation

branching off the central section of them (indicated by the white dashed circle in Fig. 5(d)). Fig. 5(e) present the morphology of products obtained when the ultrasonic irradiation time is 20 min, uncompleted flower-like CuO microstructures are found. When the ultrasonic irradiation time is prolonged to 40 min, elegant CuO microflowers are successfully achieved (Fig. 3).

Based on the above experimental facts, the growth process of flower-shaped CuO architectures is described as Fig. 6. First, under the condition of ultrasonic irradiation, CuO primary nuclei are generated by the dehydration of preformed $Cu(OH)_4^{2-}$ and rapidly developed into shuttle-like monomers, which can act as the body for the following secondary nucleation and growth . Second, possibly due to existing high active sites at the central part of CuO nanoshuttles, secondary nucleation and growth of shuttle-like nanosheets would firstly take place on these active sites, and nanoshuttles with nanosheets standing on their surfaces were produced. Third, with the prolongation of reaction time, secondary nucleation and growth of shuttle-like nanosheets would also occur at the other places on the surfaces of shuttle-like body, forming uncompleted flower-like CuO microstructures. Finally, in the later growth stage, the concentration of reactant is decreased, which could not satisfy the growth of shuttle-like nanostructures and lead to the formation of sheet-like petals with acicular tips. Through the unceasing process of oriented aggregation growth and Ostwald ripening, beautiful peony-shaped CuO architectures have been acquired.

3.3 Optical property

Fig. 7a is the UV-vis diffuse reflectance spectrum of as-prepared CuO flower-shaped microstructures, which indicates that there is a wide absorption from 200 nm to 800 nm. According to the equation $\alpha E_{photon}=K(E_{photon}-E_g)^{n/2}$, where α is the absorption coefficient, E_{photon} is the discrete photo energy, K is a constant and E_g is the band gap energy. [19] For the CuO, the value of n is 1 for the direct conductor. Fig. 7b is the $(\alpha E_{photon})^2 \sim E_{photon}$ curve of CuO microflowers. The value of optical band gap E_g is estimated to be 2.3eV, similar to CuO sheet-like nanostructures (2.31eV) reported by Wang's group, [20] greater than the value for bulk CuO (1.2eV). [7] Owing to the band gap energy in the visible region, the as-prepared hierarchical CuO microflowers may have visible-light-driven photocatalytic activity on the degradation of some organic pollutants.

3.4 Photocatalytic performance

The photocatalytic performance of as-prepared hierarchical CuO microflowers was evaluated through the degradation of organic dyes in water under visible light irradiation. Rhodamine B (RhB) was selected as a model organic pollutant for detail discussion. Fig. 8(a) shows the typical absorption spectra of RhB solution detected at different intervals using CuO microflowers as photocatalyst assisted by a small amount of hydrogen peroxide (H_2O_2). The adsorption rate of RhB on as-prepared CuO is 5.8% in 60 min under dark condition. The intensity of the characteristic absorption peak at 554 nm decreases rapidly within the initial 10 min irradiation, and the degradation rate of RhB is about 50.6%. The intense pink color of the

starting RhB solution almost completely fades after 80 min, suggesting the efficient decomposition of RhB into CO_2 and H_2O. For comparison, series of tests were carried out under different conditions, and the results are showed in Fig. 8(b). For the blank experiment, direct photolysis of RhB could almost be neglected. Only in the presence of H_2O_2, the degradation rate is 9.7 % in 80 min. It is suggested that H_2O_2 may to some extent combine with photon and generate ·OH radicals, [21] which can oxide RhB molecules. Only in the presence of CuO, about 14.7% RhB was decomposed in 80 min. The lower decolorization rate of RhB only over CuO is possibly due to the fast recombination of photogenerated electron-hole pairs in CuO crystals. However, the degradation rate of RhB over as-prepared CuO microflowers can reach 94% within 80 min with the assistance of 0.1 mL H_2O_2. For comparison, the degradation process of RhB over commercial CuO was also detected under the same conditions with as-prepared CuO. One can see that the degradation rate of RhB is only 10.1% within the initial 10 min irradiation and about 59.3% RhB was decomposed in 80 min. By comparing as-prepard CuO with commercial CuO, a conclusion can be drawn that as-prepared hierarchical CuO microflowers have the stronger ability to quickly photocatalytic degradation of organic dyes. We think the main reason is that CuO microflowers built by thin nanosheets with needle-like tips may have more active surface sites for photocatalytic reaction.

In addition, the photocatalytic performance of as-prepared hierarchical CuO microflowers was also evaluated through the degradation of Methylene blue (MB) and Methyl orange (MO)

under the same conditions, as shown in Figs. 8(c) and (d). It is found that the characteristic absorption peak of MB at 665 nm almost disappeared after irradiation for 80min, but the characteristic absorption intensity of MO at 464 nm is still stronger. The removal efficiency of MB and MO is about 96% and 41%, respectively. The comparative experiment results indicate that the as-prepared CuO catalyst obviously has selectivity of dyes, which show high photocatalytic efficiency for RhB and MB.

On the base of above series of comparative experiments, we think the appropriate combination of CuO and H_2O_2 is crucial to enhance the photocatalytic reaction efficiency. According to report, H_2O_2 is suggested to be a better photogenerated electron acceptor than oxygen to reduce the chances of electron-hole pairs recombination. [22] Under the light illumination, the electrons in CuO crystals transit from the valence band (VB) to the conduction band (CB) and leave the holes in VB, producing photogenerated electron-hole pairs. As an outstanding electron-capturing agent, the dissolved H_2O_2 adsorbed on the surface of catalyst rapidly combine with photogenerated electrons (e^-_{CB}) and produce ·OH radicals, prolonging the lifetime of photo-induced carriers. Due to its stronger oxidation capacity, the new-produced ·OH radicals can effectively oxidize RhB molecules into carbon dioxide and water. The schematic diagram of band structure in the CuO crystal is illustrated in Fig. 9. Additionally, It is reported that the active sites of the surfaces of CuO may also catalyze the decomposition of H_2O_2 to generate free radical species as • OH , • OOH and O_2 • $^-$,[23] also resulting in the enhancement of

photocatalytic efficiency.

4. Conclusions

In conclusion, we have prepared hierarchical CuO microflowers via a simple ultrasound-assisted aqueous chemical method. The sizes of CuO microflowers are estimated to be 2-3 μm. These flower-like architectures are self-assembled by CuO nanosheets with needle-like tips radiating from their center. The use of ammonia and reactive time has great effects on the phase purity and morphology development of the products. The mechanism of oriented aggregation growth and Ostwald ripening was suggested for explaining the formation of CuO hierarchical microflowers. Photocatalytic performance results indicate that the as-prepared CuO microflowers obviously have selectivity of dyes, showing high photocatalytic efficiency for RhB and MB in short time.

Acknowledgements

This work was supported by the Natural Science Foundation of Anhui Educational Committee (KJ2014ZD08) and the Fifth Science and Technology Foundation of Outstanding Youth of Anhui Province (1308085JGD06, 10040606Y25).

References

1. Moore, J. S. and Kraft, M. L. 2008. *Science*, 320: 620

2. Liu, B. and Zeng, H. C. 2005. *J. Am. Chem. Soc.*, 127: 18262

3. Peng, S. and Sun S. H. 2007. *Angew. Chem. Int. Ed.*, 46: 4155

4. Cai, W. Q., Yu, J. G., Gu, S. H. and Jaroniec, M. 2010. *Cryst. Growth Des.*, 10: 3977

5. Bae, Y., Kim, N. H., Kim, M., Lee, K.Y. and Han, S.W. 2008. *J. Am. Chem. Soc.*, 130: 5432.

6. Wen, X., Xie, Y. T., Mak, M. W. C., Cheung, K.Y., Li, X. Y., Renneberg, R., and Yang S. 2006. *Langmuir*, 22: 4836.

7. Zhu, Y. X., Wang, Y. L., Song, L.Y., Chen, X., Liu, W. Y., Sun, J., She, X.L., Zhong, Z. Y. and Su, F. B. *RSC Adv.*, 2013. 3: 9794

8. Meng, F. N., Di, X. P., Dong, H. W., Zhang, Y., Zhu, C. L., Li, C. and Chen, Y. J. 2013. *Sensor. Actuat. B: Chem*, 182: 197

9. Zhang, Y. X., Li, F. and Huang, M. 2013. *Mater. Lett.*, 112: 203.

10. Zaman, S., Zainelabdin, A., Amin, G., Nur, O. and Willander, M. 2012. *J. Phys. Chem. Solids*, 73: 1320.

11. Shi H. X., Zhao, Y. X., Li, N., Wang, K., Hua, X., Chen, M. D. and Teng, F. 2014. *Catal. Commun.*, 47: 7

12. Zhang, Z. L., Chen H., She, X. L., Sun, J., Teo, J. and Su, F .B. 2012. *J. Power Sources*, 217:

336

13. Hu, C. Y., Guo, J. and Wen, J. 2012. *Ionics*, 19: 253

14. Hu, Y. Y., Huang, X. T., Wang, K., Liu, J. P., Jiang, J., Ding, R. M., Ji, X. X. and Li, X. 2010. *J. Solid State Chem.*, 183: 662

15. Li, J. Y., Xiong, S. L., Xi, B. J., Li, X. G. and Qian, Y. T. 2009. *Cryst. Growth Des.*, 9: 4108

16. Li, J. Y., Xiong, S.L., Pan, J. and Qian, Y.T. 2010, J. Phys. Chem. C, 114: 9645

17. Gao, D. Q., Yang, G. J., Li, J. Y., Zhang, J., Zhang, J. L. and Xue, D.S. 2010. *J. Phys. Chem. C*, 114: 18347

18. Xu, Y. Y., Chen, D. R., Jiao, X. L. and Xue, K. Y. 2007. *Mater. Res. Bull.*, 42: 1723

19. Zhu, J. W., Chen, H. Q., Liu, H. B., Yang, X. J., Lu, L. D. and Wang, X. 2004. *Mater. Sci. Eng. A*, 384: 172

20. Wang, L. J., Zhou, Q., Liang, Y. J., Shi, H. L., Zhang, G. L., Wang, B. S., Zhang, W.W., Lei, B. and Wang, W. Z. 2013. *Appl. Surf. Sci.*, 271: 136

21. Wu, C. L., Shemer, H. and Linden, K.G. 2007. *J. Agric. Food Chem.*, 55: 4059.

22. Ilisz, I., Foglein, K. and Dombi, A., 1998. *J. Mol. Catal. A: Chem.*, 135: 55.

23. Zaman, S., Zainelabdin, A., Amin, G., Nur, O. and Willander, M. 2012. *J. Phys. Chem. Solids*, 73:1320

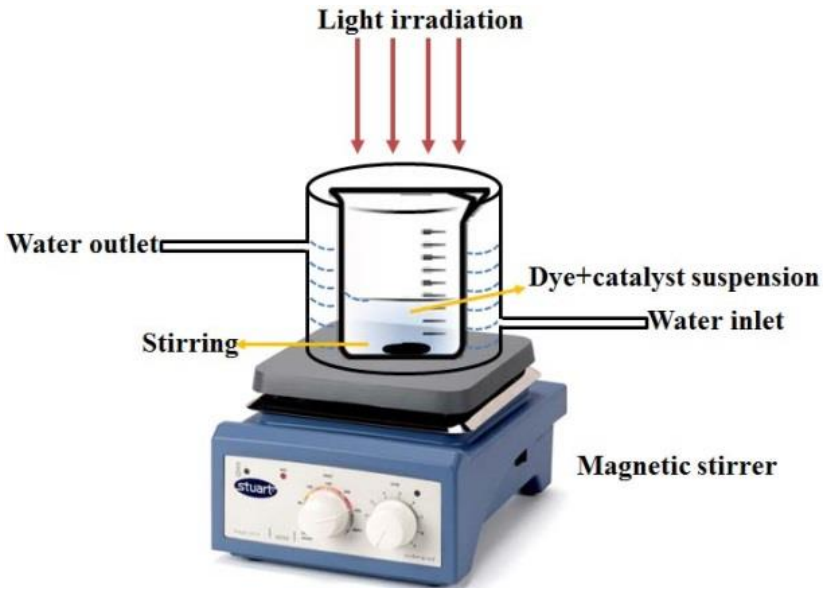

Fig. 1

Apparatus of photocatalytic experiment

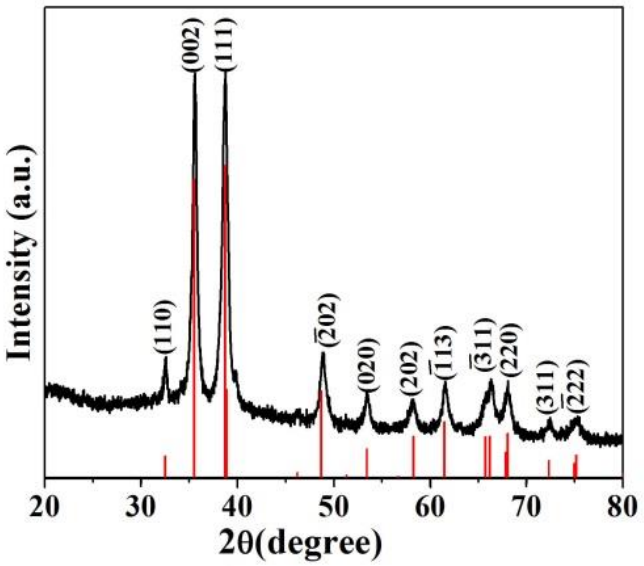

Fig. 2

XRD pattern of the as-prepared sample

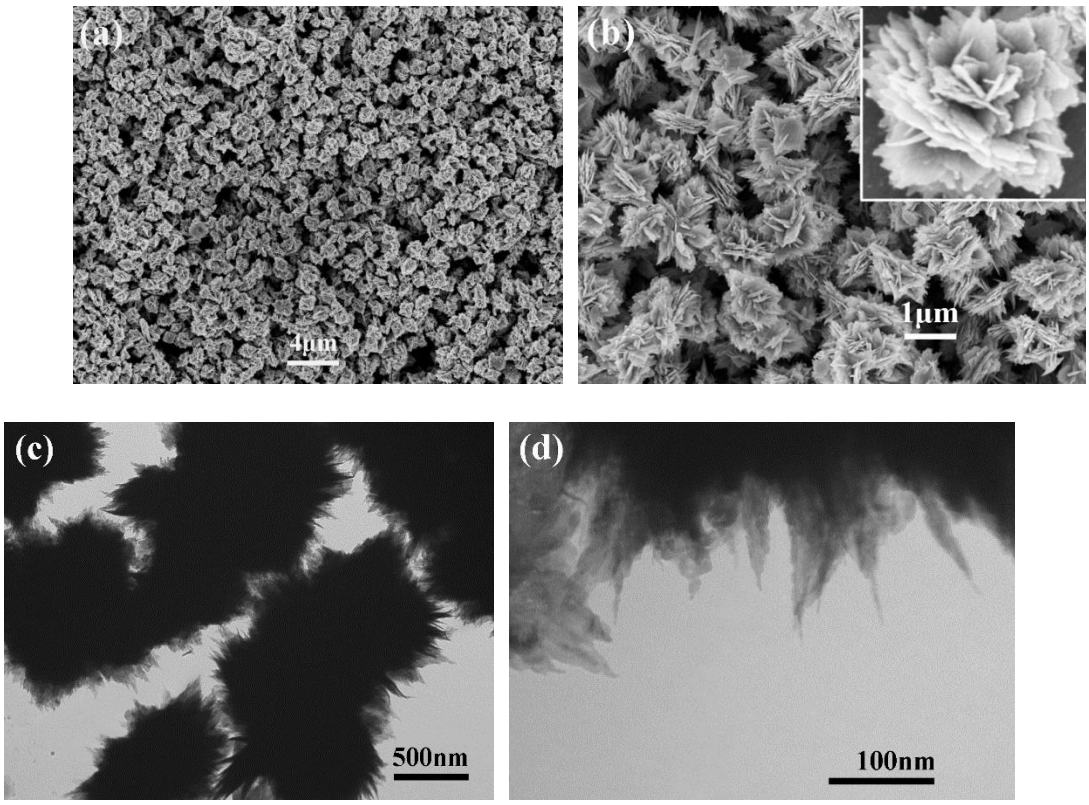

Fig. 3

FESEM images of CuO flowers products recorded at different magnification

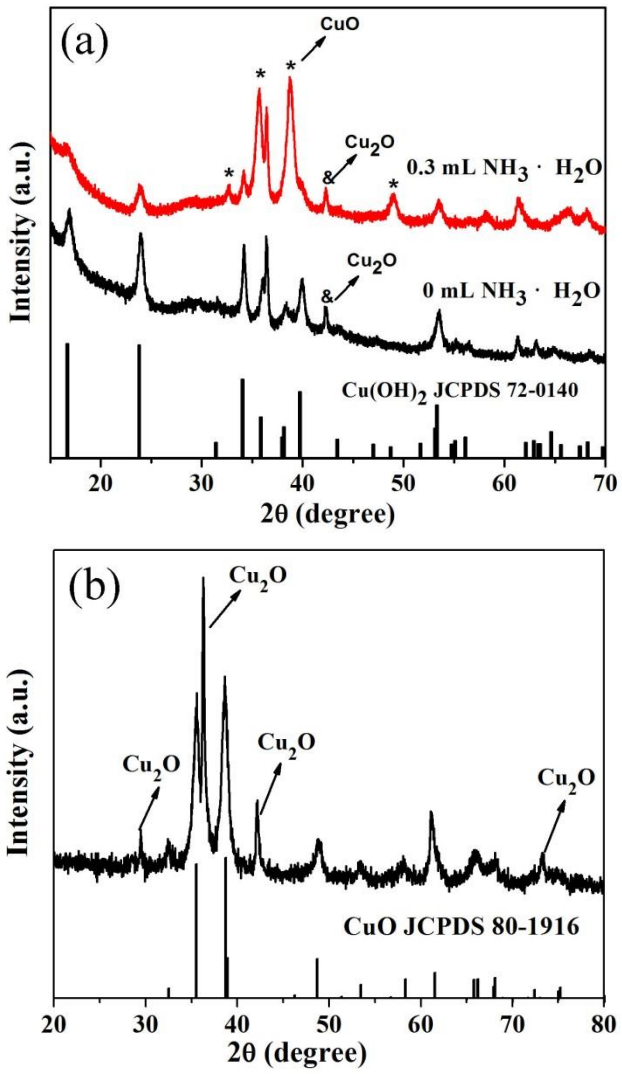

Fig. 4

(a) XRD patterns of samples obtained with different adding volume of ammonia under the condition of ultrasonic irradiation, (b) XRD pattern of product prepared without ultrasonic treatment keeping other condition constant

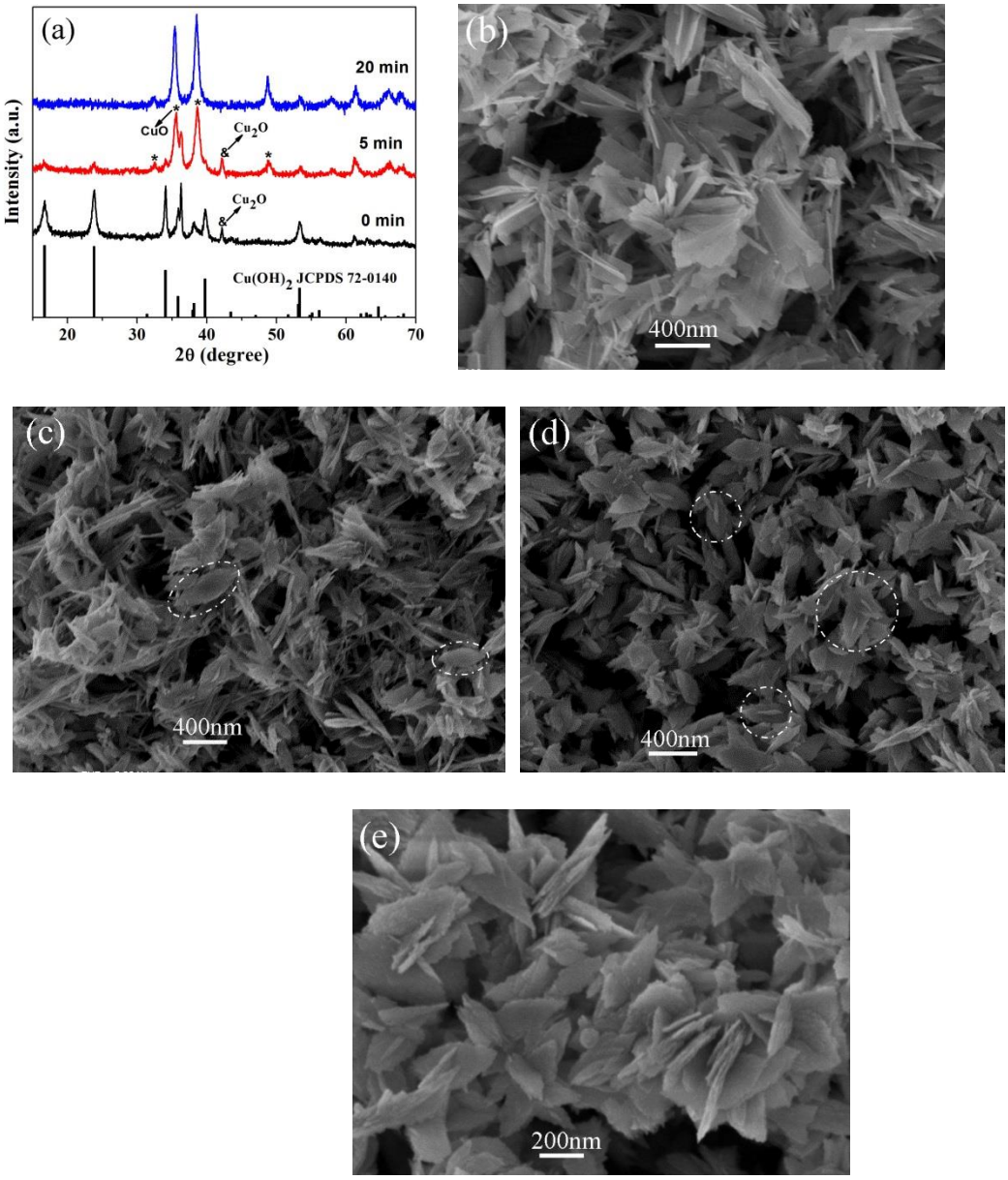

Fig. 5

(a) XRD patterns of products obtained with ultrasonic irradiation time of 0, 5 and 20 min, (b-e) FESEM images of the obtained sample at different growth stages: (b) 0min, (c) 5min, (d) 10min, (e) 20 min

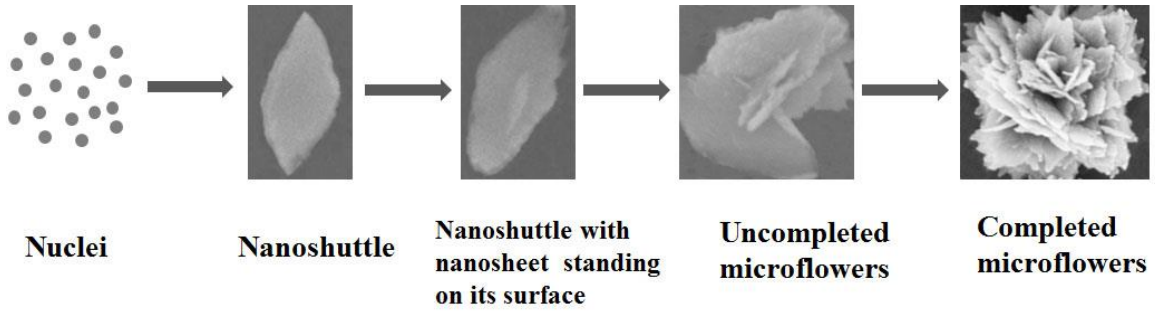

Fig. 6

Schematic illustration of the growth process for flower-shaped CuO microstructure

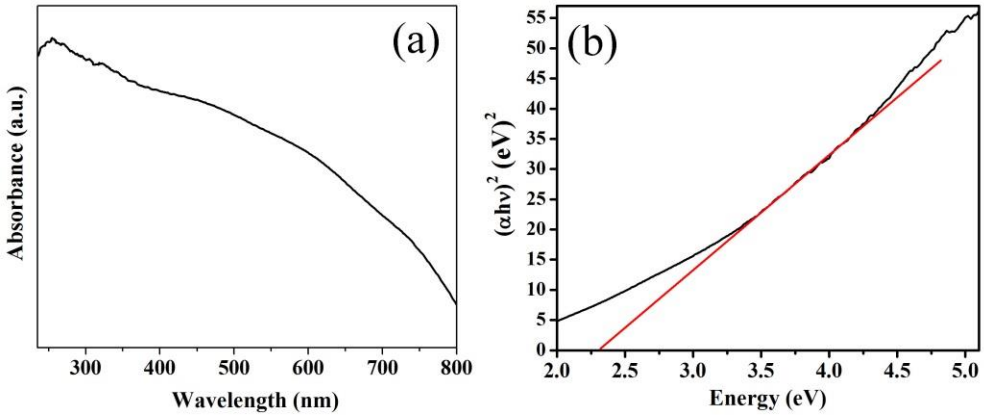

Fig. 7

(a) UV-vis absorption spectrum and (b) $(\alpha h\upsilon)^2 \sim h\upsilon$ curve of CuO flower-shaped architectures

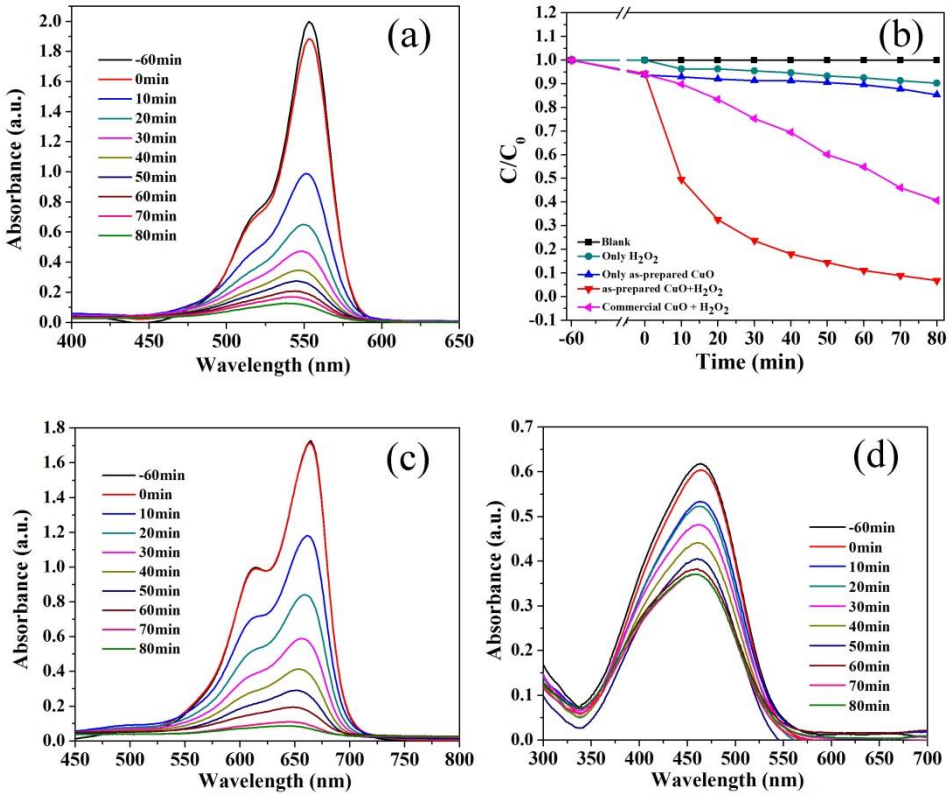

Fig.8

(a) Photodegradation process of RhB over CuO microflowers in the presence of H_2O_2, (b) Degradation rate of RhB at different intervals under different conditions, (c) Photodegradation process of MB over CuO microflowers in the presence of H_2O_2, (d) Photodegradation process of MO over CuO microflowers in the presence of H_2O_2

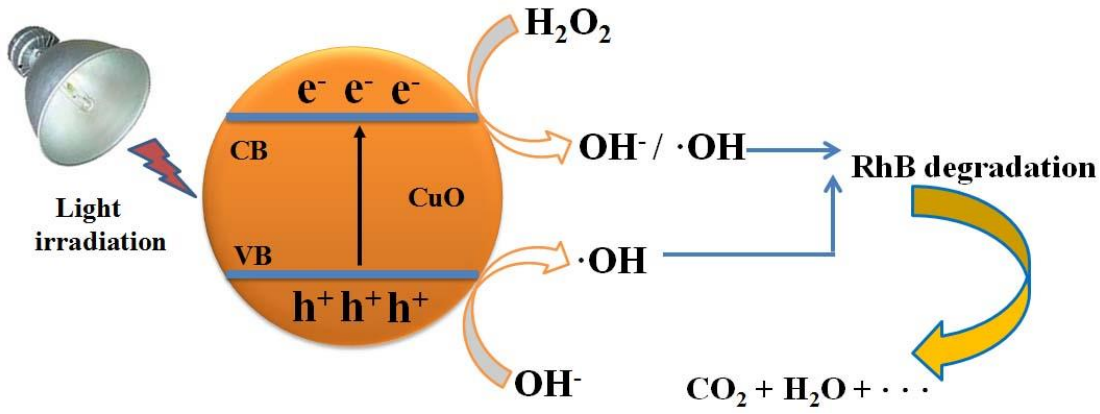

Fig. 9

Schematic diagram of band structure in the CuO crystal